Natural Attenuation of Mn(II) in Metal Refinery Wastewater: Microbial Community Structure Analysis and Isolation of a New Mn(II)-Oxidizing Bacterium Pseudomonas sp. SK3

Kitjanukit, Santisak
Department of Earth Resource Engineering, Faculty of Engineering, Kyushu University

Takamatsu, Kyohei
Department of Earth Resource Engineering, Faculty of Engineering, Kyushu University

Okibe, Naoko
Department of Earth Resource Engineering, Faculty of Engineering, Kyushu University

出版情報：Water. 11 (3), pp.507-, 2019-03-11. MDPI
バージョン：

water

MDPI

Article

Natural Attenuation of Mn(II) in Metal Refinery Wastewater: Microbial Community Structure Analysis and Isolation of a New Mn(II)-Oxidizing Bacterium *Pseudomonas* sp. SK3

Santisak Kitjanukit, Kyohei Takamatsu and Naoko Okibe *

Department of Earth Resource Engineering, Faculty of Engineering, Kyushu University, 744 Motooka, Nishi-ku, Fukuoka 819-0395, Japan; ming@mine.kyushu-u.ac.jp (S.K.); k-takamatsu16@mine.kyushu-u.ac.jp (K.T.)

Received: 7 February 2019; Accepted: 5 March 2019; Published: 11 March 2019

Abstract: Natural attenuation of Mn(II) was observed inside the metal refinery wastewater pipeline, accompanying dark brown-colored mineralization (mostly $Mn^{IV}O_2$ with some $Mn^{III}{}_2O_3$ and Fe_2O_3) on the inner pipe surface. The Mn-deposit hosted the bacterial community comprised of *Hyphomicrobium* sp. (22.1%), *Magnetospirillum* sp. (3.2%), *Geobacter* sp. (0.3%), *Bacillus* sp. (0.18%), *Pseudomonas* sp. (0.03%), and non-metal-metabolizing bacteria (74.2%). Culture enrichment of the Mn-deposit led to the isolation of a new heterotrophic Mn(II)-oxidizer *Pseudomonas* sp. SK3, with its closest relative *Ps. resinovorans* (with 98.4% 16S rRNA gene sequence identity), which was previously unknown as an Mn(II)-oxidizer. Oxidation of up to 100 mg/L Mn(II) was readily initiated and completed by isolate SK3, even in the presence of high contents of $MgSO_4$ (a typical solute in metal refinery wastewaters). Additional Cu(II) facilitated Mn(II) oxidation by isolate SK3 (implying the involvement of multicopper oxidase enzyme), allowing a 2-fold greater Mn removal rate, compared to the well-studied Mn(II)-oxidizer *Ps. putida* MnB1. Poorly crystalline biogenic birnessite was formed by isolate SK3 via one-electron transfer oxidation, gradually raising the Mn AOS (average oxidation state) to 3.80 in 72 h. Together with its efficient in vitro Mn(II) oxidation behavior, a high Mn AOS level of 3.75 was observed with the pipeline Mn-deposit sample collected in situ. The overall results, including the microbial community structure analysis of the pipeline sample, suggest that the natural Mn(II) attenuation phenomenon was characterized by robust in situ activity of Mn(II) oxidizers (including strain SK3) for continuous generation of Mn(IV). This likely synergistically facilitated chemical Mn(II)/Mn(IV) synproportionation for effective Mn removal in the complex ecosystem established in this artificial pipeline structure. The potential utility of isolate SK3 is illustrated for further industrial application in metal refinery wastewater treatment processes.

Keywords: manganese; natural attenuation; Mn(II)-oxidizing bacteria; microbial community structure; *Pseudomonas*

1. Introduction

Soluble Mn(II) ions persist in a wide pH range and, thus, their removal from mining-impacted waters is a challenging task. For its removal, Mn(II) needs to be oxidized to Mn(III) or Mn(IV), which precipitate as dark brown Mn-oxides. Although metal refinery wastewaters and mining-impacted drainages are often acidic, conventional chemical Mn(II) oxidation requires alkaline pH conditions (and, thus, a large input of neutralizing agents) to overcome the thermodynamic barrier [1]. On the other hand, the use of Mn(II)-oxidizing microorganisms enables enzymatic Mn(II) oxidation at circumneutral pHs, without the addition of chemical oxidizing agents [2]. Therefore, the development of a

bioprocess for Mn(II)-contaminated waters could become a more economical and environmentally feasible alternative.

Mn(II)-oxidizing bacteria are phylogenetically diverse, including Firmicutes (*Bacillus* sp. *Brevibacillus* sp.), Proteobacteria (*Leptothrix* sp., *Pseudomonas* sp., *Erythrobacter* sp., *Pedomicrobium* sp.) and Actinobacteria (*Arthrobacter* sp.) [2,3]. The presence of multicopper oxidase (MCO; at least four copper atoms present as cofactor) was reported in these bacteria as Mn(II) oxidase enzyme, exemplified by MnxG (*Bacillus* sp. SG-1 [4]), CopA (*Brevibacillus panacihumi* MK-8 [5]), MofA (*Leptothrix discophora* SS-1 [6]), CumA (*Ps. putida* GB-1 [7]), and MoxA (*Pedomicrobium* sp. ACM 3067 [8]). More recently, the involvement of an animal heme peroxidase (AHP) in Mn(II) oxidation was found in *Ps. putida* GB-1, showing the first example of an Mn(II)-oxidizing bacterium utilizing both MCO and AHP enzymes [9].

Different types of Mn-oxides were reported as a result of microbial Mn(II) oxidation, including birnessite ($(Na, Ca)_{0.5}(Mn^{IV}, Mn^{III})_2O_4 \cdot 1.5H_2O$), todorokite ($(Mn^{II}, Ca, Na, K)(Mn^{IV}, Mn^{II}, Mg)_6O_{12} \cdot 3H_2O$), bixbyite ($(Mn^{III}, Fe^{III})_2O_3$), and hausmannite ($Mn^{II}, Mn^{III}{}_2O_4$), formed by bacteria and fungi [3,10–13]. It was suggested that birnessite-like biogenic Mn-oxides are initially formed enzymatically, and later transformed into lower average oxidation state (AOS) Mn-oxides, such as hausmannite, due to reaction with the remaining Mn(II) or crystallized to todorokite [14,15].

Unlike for Fe(II)-oxidizing bacteria, the reason why Mn(II)-oxidizing bacteria oxidize Mn(II) is still unclear. Although the oxidation of Mn(II) to Mn(III) or Mn(IV) is thermodynamically favorable, there is no direct evidence linking Mn(II) oxidation to energy conservation [3]. The possible advantages of microbial Mn(II) oxidation could include storage of Mn-oxides as an electron acceptor and self-protection by Mn-oxide armoring from environmental insults (e.g., UV, predation, toxic heavy metals). Also, since Mn-oxide is one of strongest oxidants found in nature, Mn(II)-oxidizing bacteria may benefit from its capability to degrade recalcitrant humic substances into low molecular organic compounds for feeding [2,3].

Nonetheless, regardless of which mechanism is involved in microbial Mn(II) oxidation, the activity of such Mn(II)-oxidizing bacteria have been widely observed not only in natural open environments, but also within artificial structures, such as freshwater pipelines and sewage treatment plants [16–19]. The majority of naturally occurring Mn-oxides in these environments are considered to originate directly from microbial Mn(II) oxidation or from the subsequent alteration of biogenic Mn-oxides [3]. This indicates the ubiquitous and robust nature of these Mn(II)-oxidizing bacteria, resulting in an extensive impact on the Mn geochemistry of the earth's crust.

The motivation for this study arose from the discovery of natural Mn(II) attenuation in metal refinery wastewater, which was accompanied by extensive mineralization on the inner surface of the wastewater pipeline. Based on the pH and ORP values of the wastewater, this phenomenon appeared to involve biological intervention, rather than spontaneous chemical Mn(II) oxidations. The mechanism of this natural Mn(II) attenuation could be reconstituted as a bioprocess to be introduced in wastewater treatment facilities.

So far, utilization of such an Mn(II) removal bioprocess has been reported for the treatment of ground and drinking waters with Mn(II) concentrations ranging from <1 mg/L to a few mg/L at neutral pHs, mostly exemplified by sand biofilters [20–23]. In metal refinery industries, the Mn(II)-oxidizing bioprocess should ideally be introduced further upstream in the water treatment system. Generally, highly acidic metal refinery waters are first alkalized to facilitate chemical Mn(II) oxidation to remove Mn-oxide precipitates. The bioprocess could be potentially installed as a post-treatment following the neutralization step, in order to reduce the vast cost for alkaline agents. For this aim, it was necessary to find an isolate which withstands high Mn(II) concentrations and displays robust Mn(II) oxidation, especially in the presence of $MgSO_4$ as a typical major component in refinery wastewaters. This study reports microbial and chemical analyses of the natural Mn(II) attenuation phenomena in the metal refinery wastewater pipeline, and isolation and characterization of a new Mn(II)-oxidizing bacterium with a robust Mn(II)-oxidizing capability.

2. Materials and Methods

2.1. Collection and Analysis of On-Site Samples

2.1.1. Water Samples

Mn(II)-containing wastewater samples were collected at the inlet and outlet of the wastewater pipe in the metallurgical wastewater treatment facility. The pH and ORP values were measured on-site. Concentrations of metals, NO_3^-, and TOC (total organic carbon) were determined by ICP-OES (iCAP 6500, Thermo Scientific, Waltham, MA, USA), ion chromatography (Dionex ICS1000, Thermo Scientific), and TOC analyzer (TOC-5000A, Shimadzu, Kyoto, Japan), respectively.

2.1.2. Mn-Deposit Sample

Dark-brown-colored precipitates that had accumulated on the inner surface of the wastewater pipe were collected. An aliquot of the freeze-dried sample was digested with 60% HNO_3 (for TOC analysis), or with aqua regia (HNO_3:HCl = 3:1, for metal composition) in Teflon vessels placed in the microwave digestion system (Ethos Plus, Milestone, Sorisole, Italy) (heated to 210 °C with 7 °C/min increments, kept for 15 min at 210 °C, and finally allowed to cool to room temperature). The sample was then filtered (0.22 μm) and diluted (with deionized water) for the TOC (TOC-VCHS, Shimadzu) and ICP-OES (Optima 8300DV, PerkinElmer, Waltham, MA, USA) analyses.

The freeze-dried Mn-deposit sample was also analyzed by X-ray diffraction (XRD; Ultima IV, Rigaku, Tokyo, Japan; CuKα 40 mA, 40 kV) and by X-ray absorption near edge structure (XANES) to calculate the Mn oxidation states (as described in 2.4.2). Genomic DNA was extracted from the fresh Mn-deposit sample, and next-generation sequencing was performed to analyze the microbial community structure based on the 16S rRNA gene sequence (Techno Suruga Lab. Co. Ltd., Shizuoka, Japan). The gene sequences obtained were compared with those from GenBank using the BLAST search tool (http://blast.ncbi.nlm.nih.gov/Blast.cgi).

2.2. Isolation, Identification, and Construction of a Phylogenetic Tree for the New Mn(II)-Oxidizing Bacterium

An aliquot of the Mn-deposit sample was diluted 10 times with 0.85% (w/v) NaCl, 100 μL of which was spread onto the following solid media containing 10 mg/L Mn(II) (as $MnCl_2$): Yu medium (4.5 g/L PIPES, 2.43 mM $MgSO_4 \cdot 7H_2O$, 0.48 mM $CaCl_2 \cdot 2H_2O$, 0.005% peptone, 15 g/L agarose; pH 7.0), K medium (20 mM PIPES, artificial seawater, 0.05% yeast extract, 0.02% peptone, 15 g/L agarose; pH 7.0), and J medium (20 mM PIPES, artificial seawater, 1.5 mM NH_4Cl, 2 mM $KHCO_3$, 73 μM KH_2PO_4, vitamin mix, 0.5% methanol, 15 g/L agarose; pH 7.0). Plates were incubated at 25 °C for 3 days until brown colonies appeared (indicator for Mn(II)-oxidizing activity). After repeating single-colony isolation four times, four isolates (SK1 from K medium; SK2-3 from Yu medium, SK4 from J medium) were tested for Mn(II) oxidation ability in respective liquid media containing 100 mg/L Mn(II). As a result, only isolate SK3 exhibited stable Mn(II)-oxidizing ability during subculturing. Except for Mn(II) oxidation tests, isolate SK3 was maintained in lysogeny broth (LB) medium.

Genomic DNA was extracted from SK3 cells using the UltraClean Microbial DNA Isolation Kit (MO-BIO), and the partial 16S rRNA gene was amplified by Touchdown PCR (Premix Taq, Takara BIO) using universal 27F (5′-AGAGTTTGATCMTGGCTCAG-3′) and 1492R (5′-TACGGYTACCTTGTTACGACTT-3′) primers [16]. The PCR product was purified (Mono FAS, GL Sciences), sequenced (Research Support Center, Graduate School of Medical Sciences, Kyushu University), and analyzed by BLAST (http://blast.ncbi.nlm.nih.gov/Blast.cgi). The phylogenetic tree was constructed using the neighbor-joining method with a bootstrap value of 1000 using ClustalX v2.0 [24] and visualized by NJplot software.

2.3. Mn(II) Oxidation Test

In addition to the new isolate *Pseudomonas* sp. SK3, the well-studied Mn(II)-oxidizing relative, *Ps. putida* MnB1 (ATCC 23483), was also tested as a comparison. Each strain was pre-grown overnight in LB medium (pH 7.0), washed, and harvested by centrifugation prior to use in the following Mn(II)oxidation experiments.

In all cases, duplicate flasks were set up and incubated with shaking at 120 rpm. Samples were routinely withdrawn to monitor cell density (bacterial counting chamber), pH, and Mn(II) concentration (ICP-OES).

2.3.1. Effect of Initial Mn(II), Cu(II), and $MgSO_4$ Concentrations

Pre-grown cells were resuspended (1×10^9 cells/mL) into 300 mL Erlenmeyer flasks containing 100 mL of PYG-1 medium (1 mM glucose, 0.025% yeast extract, 0.025% peptone, 2.02 mM $MgSO_4 \cdot 7H_2O$, 0.068 mM $CaCl_2 \cdot 2H_2O$, 15 mM PIPES). The initial Mn(II) concentration was set at 100 or 200 mg/L (added as $MnSO_4$), with or without additional 3 μM Cu(II) (added as $CuCl_2$). Next, in addition to 24 mg/L $MgSO_4$ originally present in PYG-1 medium, its initial concentration was raised to 240, 1200, or 2400 mg/L to see the effect of excess $MgSO_4$ on microbial Mn(II) oxidation (3 μM Cu(II) was added in all cases). The initial pH value was set to 7.0 and temperature at 25 °C.

2.3.2. Effect of pH and Temperature

Pre-grown cells were resuspended (1×10^9 cells/mL) into 300 mL Erlenmeyer flasks containing 100 mL of PYG-1 medium. The initial Mn(II) concentration was set at 100 mg/L, plus 3 μM Cu(II). The initial pH was set at 6.0, 6.5, 7.0, 7.5, or 8.0 (25 °C), and temperature at 20, 25, 30, 35, or 40 °C (pH 7.0).

2.3.3. Effect of Individual PYG-1 Medium Components (Test for Isolate SK3 Only)

In order to investigate the durability of microbial Mn(II) oxidation in oligotrophic medium, pre-grown SK3 cells were resuspended (1×10^9 cells/mL) into 300 mL flasks containing 100 mL of PYG-1 medium lacking single/multiple organic components as follows: −Glu, −YE/Pep, −Glu/YE/Pep, −Pep (YE 0.01% instead of 0.025%) (Glu, glucose; YE, yeast extract; Pep, peptone). In addition, the effect of the absence of PIPES was also evaluated (−PIPES). The initial Mn(II) concentration was set at 100 mg/L plus 3 μM Cu(II). The initial pH value was set at 7.0 and the temperature at 25 °C.

2.4. Characterization of Biogenic Mn-Precipitates

2.4.1. X-ray Diffraction (XRD)

Biogenic Mn-precipitates were periodically collected by centrifugation during Mn(II) oxidation by isolate SK3 (at 0, 24, 48, and 72 h). The precipitates were washed with deionized water twice and freeze-dried overnight for XRD analysis (Ultima IV, Rigaku, Tokyo, Japan; CuKα 40 mA, 40 kV). Standard acid birnessite sample was chemically synthesized as described in [25].

2.4.2. X-ray Absorption Near Edge Structure (XANES)

Biogenic Mn-precipitates were collected during Mn(II) oxidation by isolate SK3 (as described in 2.4.1.) as well as by *Ps. putida* MnB1 (at 0, 24, 48, 72). Each sample was quantitatively mixed with boron nitride and pressed into a tablet. The Mn K-edge XANES spectra were collected (transmission mode; 6200–8500 eV) at SAGA-LS (1.4 GeV, 75.6 m; Kyushu University Beam Line 06), using standard chemicals $Mn^{II}SO_4$, $Mn^{III}{}_2O_3$, and δ-$Mn^{IV}O_2$ (Wako pure chemicals). The ratio of Mn species and the average oxidation states (AOS) were calculated based on the linear combination fitting of Mn K-edge XANES spectra (6200–6600 eV) using the Athena program (Demeter version 0.9.24) [26].

2.4.3. Scanning Electron Microscope (SEM)

Biogenic Mn-precipitates were fixed with a mixture of 2% glutaraldehyde and 2.5% formaldehyde in 0.1 M phosphate buffer solution (PBS; pH 7.6) (4 °C, 30 min), washed twice with 0.1 M PBS, dehydrated with ascending concentrations of ethanol (70%, 80%, 90%, and 99.5% for 5 min each, and 100% for 10 min), dried in vacuum desiccator for 24 h, and finally magnetron sputter-coated with Au–Pd (MSP-1S, Vacuum Device, Ibaraki, Japan), prior to SEM observation (SEM; VE-9800, Keyence, Osaka, Japan; 5 kV).

3. Results and Discussion

3.1. Analysis of On-Site Samples

The physicochemical characteristics of the wastewater and Mn-deposit samples are shown in Table 1. Compared to other solutes, the Mn(II) concentration was noticeably lowered from 1–n to 0.n mg/L as the water traveled through a wastewater pipe (Table 1). The inner pipe surface was found to be heavily encrusted with dark-brown precipitates, the typical color of Mn-oxides. In fact, the main metal constituent of the precipitate was Mn, with less abundant metals such as Fe, Ca, and Mg (Table 1) and XRD detected crystalline $Mn^{IV}O_2$, $Mn^{III}{}_2O_3$, and Fe_2O_3 (Figure 1). Owing to the neutral pH and low ORP values of the water samples (Table 1), spontaneous chemical Mn oxidation was unlikely to be triggered, and it was suspected that microbiological interaction was involved in this natural attenuation phenomenon. The linear combination fitting of Mn K-edge XANES spectra (data not shown) indicated that the ratio of Mn oxidation states of the Mn-deposit was Mn(IV) 84%, Mn(III) 13%, and Mn(II) 3%, with an average oxidation state (AOS) of 3.75.

Naturally occurring biogenic Mn-oxides are generally formed as poorly crystalline birnessite, as observed in environments such as hot springs and streambed crusts [16,27]. These primary biogenic Mn-oxides were reported to transform into different crystalline Mn-oxides (e.g., todorokite), through prolonged exposure to interlayer cations such as Mg(II), Ca(II), Ni(II), and Zn(II) [14,28]. The reaction of primary biogenic Mn-oxides (by *Bacillus* sp. SG-1) with Mn(II) was also shown to result in the abiotic formation of secondary feitknechtite ($Mn^{III}OOH$) or phyllomanganate, depending on the Mn(II) concentration [29]. Based on the water characteristics shown in Table 1, such natural transformation reactions also likely took place in the wastewater pipe during years of operation to produce crystalline Mn-oxides deposits, even though the primary products were poorly crystalline.

Table 1. Characteristics of wastewater samples (taken from the inlet and outlet of the wastewater pipe).

	Wastewater Samples		**Mn-Deposits Sample**
	Inlet	**Outlet**	
pH	7.9	7.6	-
ORP (mV)	100	105	-
TOC (mg/L)	4	ND	2.5
NO_3 (mg/L)	11	ND	ND
Metal Composition	(mg/L)		(mg/g)
Mn	1–n	0.n	617
Fe	< 0.01	< 0.01	121
Cu	< 0.01	< 0.01	0.06
Ca	389	386	59
Mg	280	276	51
Si	5.3	5.3	ND

Note: ND: Not Determined.

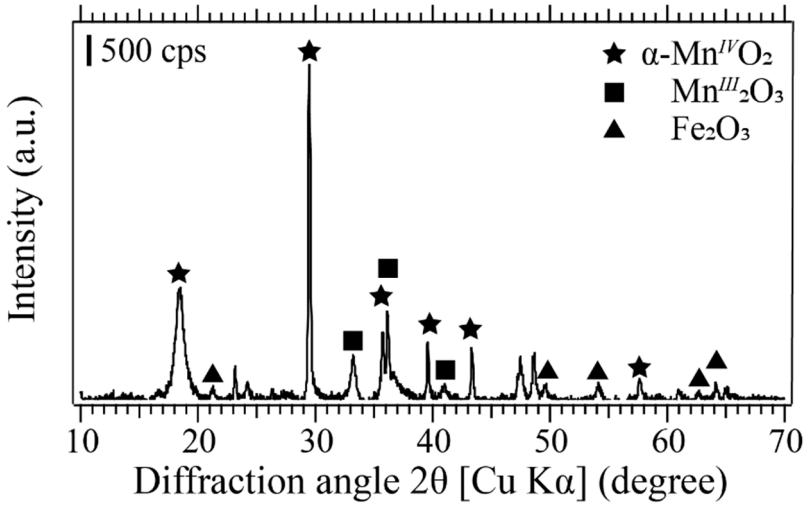

Figure 1. X-ray diffraction patterns of the Mn-deposit collected from the metal refinery wastewater pipe. ★, α-Mn^{IV}O$_2$ (JCPDS 44-141); ■, Mn$^{III}_2$O$_3$ (JCPDS 41-1442); ▲, Fe$_2$O$_3$ (JCPDS 39-1346).

3.2. Microbial Community Structure Analysis

The bacterial community structure in the Mn-deposit was analyzed in order to search for Mn(II)-oxidizing bacteria responsible for its formation in the wastewater pipe. The number of 16S rRNA gene sequences analyzed was 22,733, from which 18,605 (81.8%) were unclassified and 352 (1.5%) did not match database entries. Figure 2 shows the bacterial community structure based on the remaining 3776 (16.6%) classified sequences (the full analysis result shown in Figure S1).

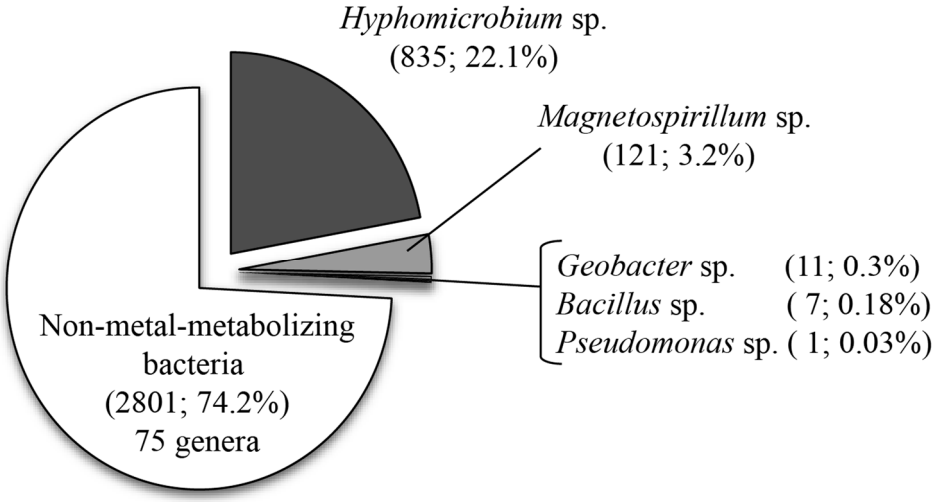

Figure 2. Bacterial community structure in the Mn-deposit collected from the metal refinery wastewater pipe. Values in brackets indicate the total number of sequences and the percentage.

Around 74.2% of the community was unknown as metal-metabolizing bacteria, the majority (52%) of which were *Porphyrobacter* spp. (Figure S1; mostly *P. sanguineus*)—they receive light energy with bacteriochlorophyll but perform aerobic photoheterotrophic metabolism requiring organic substrates for growth [30]. Since the wastewater was once pooled in open storage before entering the pipe, the photoheterotrophs may have taken advantage of the light to dominate the community in a nutrient-limiting environment.

The second dominant genus (22.1%) was aerobic, methylotrophic budding bacteria *Hyphomicrobium* (Figure 2) (mostly *H. zavarzinii* and *H. hollandicum*; Table S2), characteristic in producing hyphal filaments during growth. *Hyphomicrobium* has been widely detected as a dominant

member in Mn-deposits from worldwide locations, including freshwater pipelines [19] and sewage treatment plants [17]. Despite its abundance in Mn-deposits, the difficulty in its isolation and steady maintenance makes it still unclear whether or not *Hyphomicrobium* is indeed directly responsible for Mn(II) oxidation [19,31]. The observation that *Hyphomicrobium* are capable of autotrophic growth [32] and that they were found associating with the initial building up of Mn-deposits in the recirculatory apparatus [31] lead us to speculate upon its important role in primary colonization via a unique hyphae network onto the pipeline surface, establishing the structural and nutritional scaffolds to support secondary colonization of heterotrophic Mn(II)-oxidizers against a continuous water flow (Figure 3).

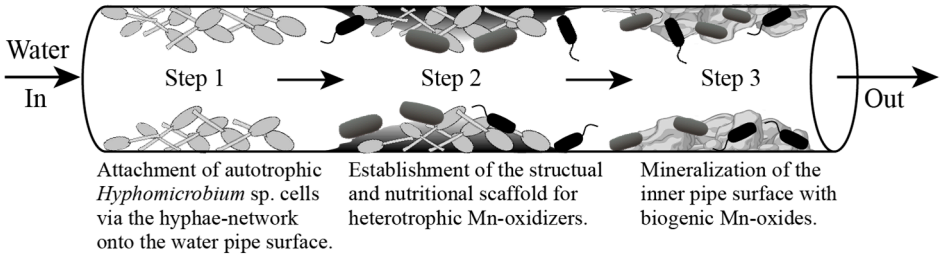

Figure 3. Schematic image of the proposed Mn-deposit formation process in the water pipe.

Microaerobic magnetotactic bacteria, *Magnetospirillum* spp. (all *Ms. gryphiswaldense*; Table S2) accounted for 3.2% of the community structure (Figure 2). *Ms. gryphiswaldense* synthesizes nanosized magnetosomes (Fe_3O_4) by active uptake and reduction of Fe^{3+} through ferric reductase [33]. Mn concentration in the wastewater may have been affected by this bacterium to some extent, since Mn can be incorporated into magnetite crystals [34].

Facultative anaerobes, *Geobacter* spp. (mostly *Gb. sulfurreducens*; Table S2), comprised 0.3% of the community (Figure 2). These Fe(III)-reducing bacteria may adversely affect Mn(II) oxidation in the wastewater pipe, as they may reduce Mn-oxides in anaerobic respiration in the event of oxygen depletion [35]. The genus *Bacillus* and *Pseudomonas* accounted for a minor portion of the community structure (0.18% and 0.03%, respectively; Figure 2). Mn(II) oxidation is well-studied in some *Bacillus* and *Pseudomonas* strains, such as *Bacillus* sp. SG-1 [36], *Ps. putida* MnB1 [25], and *Ps. putida* GB-1 [37]. From the Mn-deposit in this study, six different *Bacillus* spp. and *Ps. resinovorans* were detected (Figure S1). However, the Mn(II)-oxidizing ability is yet unknown in these species. As was proposed in Figure 3, the growth of these possible heterotrophic Mn(II) oxidizers (perhaps as well as non-Mn-metabolizing *Porphyrobacter*) may depend on the growing biofilms of *Hyphomicrobium*, by scavenging organic exudates deriving from these primary colonizers.

3.3. Isolation of Pseudomonas sp. SK3 and Its Phylogenetic Analysis

Three Mn(II)-oxidizing isolates (SK1, 2, and 3) were obtained after repeated single colony isolation. Following several rounds of subculturing and Mn(II) oxidation tests at 100 mg/L Mn(II), isolate SK3 was selected as the most stable and strongest Mn(II)-oxidizer for further studies. Based on the 16S rRNA gene sequence of isolate SK3 (1398 bp), its closest relative was shown to be *Ps. resinovorans* ATCC 14235T (AB021373) with a similarity of 98.4% (Figure 4). So far, several Mn(II)-oxidizing strains have been reported from the *Ps. putida* group. However, the presence of Mn(II) oxidation ability is so far unknown in *Ps. resinovorans* (Figure 4). Identification of *Pseudomonas* sp. SK3 implies that Mn(II)-oxidizing ability may be more diversely present across the genus *Pseudomonas*.

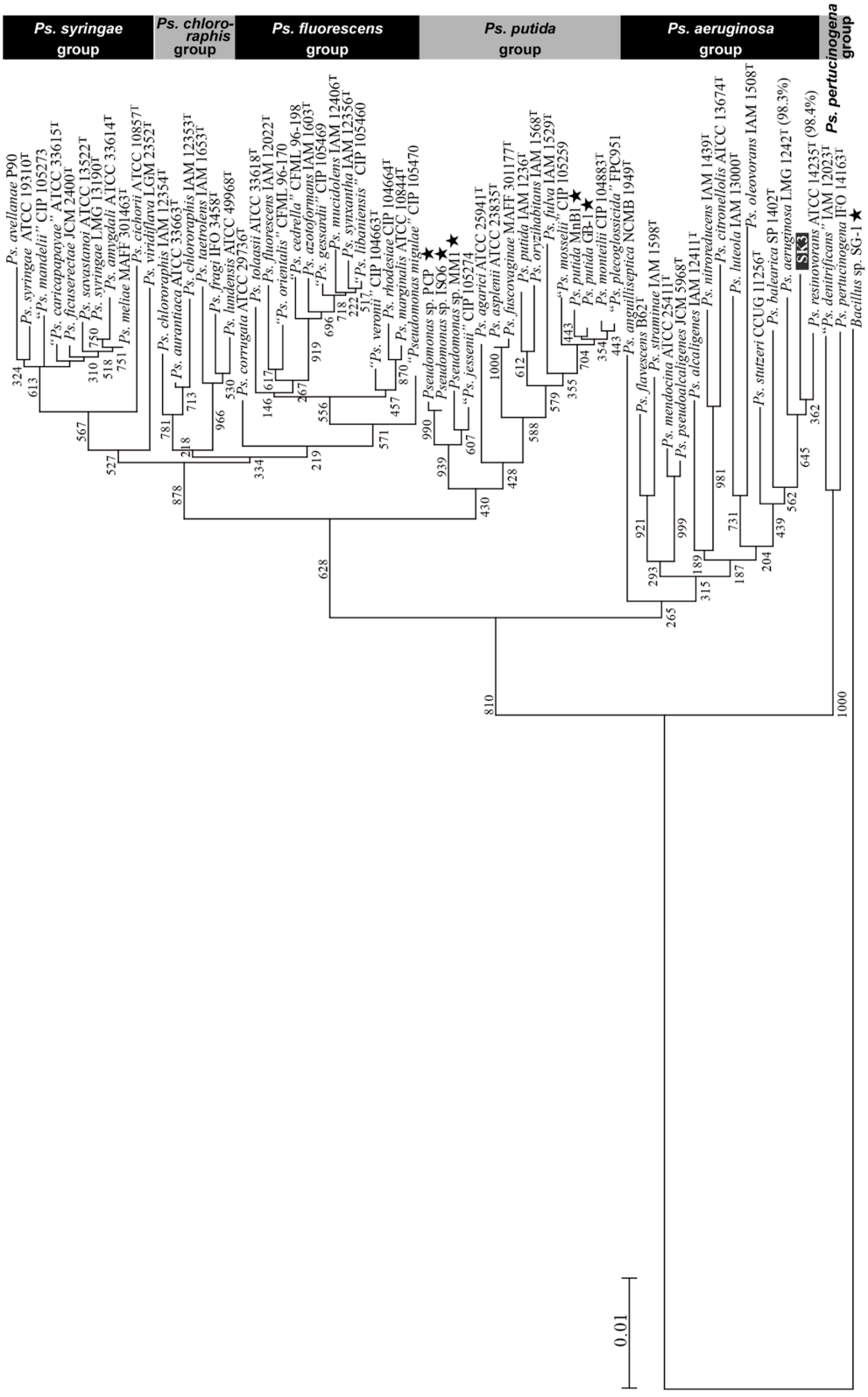

Figure 4. Phylogenetic tree of isolate SK3 in relation to known *Pseudomonas* spp., based on the 16S rRNA gene sequence, constructed by the neighbor-joining method (using *Bacillus* sp. SG1 as the outgroup). Known Mn(II)-oxidizing strains are marked (★). Scale bar indicates the number of nucleotide substitutions per site. Numbers at nodes indicate bootstrap values for 1000 replicates of the original dataset. NCBI accession numbers are summarized separately in Table S1. Numbers in brackets indicate the 16S rRNA gene sequence identities with isolate SK3.

3.4. Mn(II) Oxidation by Pseudomonas sp. SK3

3.4.1. Effect of Initial [Mn(II)], [Cu^{2+}], and [$MgSO_4$]

Our challenge in this study was to find a robust Mn(II)-oxidizer which can be potentially utilized in an industrial Mn(II) treatment process. Ideally, the new bioprocess would be placed further upstream of the metal refinery wastewater treatment system to deal with a few tens of mg/L Mn(II) contaminant coexisting with $MgSO_4$ at neutral or slightly acidic pH values.

First, pre-grown cells of isolate SK3 (as well as *Ps. putida* MnB1, a well-studied Mn(II)-oxidizer, for comparison) were tested for Mn(II) oxidation at 100 and 200 mg/L (each with or without additional 3 μM Cu(II)). As shown in Figure 5a, isolate SK3 completely oxidized 100 mg/L Mn(II) by 48 h (plus Cu(II)), while the absence of Cu(II) clearly slowed down its Mn(II) oxidation. A similar effect of Cu(II) was apparent with *Ps. putida* MnB1, but its Mn(II) oxidation was generally slower, compared to isolate SK3 (Figure 5a). When the initial Mn(II) concentration was raised to 200 mg/L, Mn(II) oxidation by *Ps. putida* MnB1 became negligible, while isolate SK3 managed to partially oxidize Mn(II), especially in the presence of Cu(II) (37 mg/L oxidized in 70 h; Figure 5a). The presence of 3 μM Cu(II) was found to be sufficient, since the addition of Cu(II) at higher concentrations (5 or 10 μM) resulted in similar Mn(II) oxidation removal efficiencies by isolate SK3 (data not shown). The results here support the hypothesis that isolate SK3 also shares the activity of MCO enzyme in Mn(II) oxidation, as was reported with *Ps. putida* GB-1 [7] as well as in other genera, such as *Bacillus* [4], *Brevibacillus* [5], and *Leptothrix* [6].

Isolate SK3 exhibited remarkable resistance to high $MgSO_4$ doses. Although an increasingly longer delay in Mn(II) oxidation was observed, corresponding to higher $MgSO_4$ doses, isolate SK3 still managed to effectively oxidize Mn(II) nearly to completion by 120 h (Figure 5b). On the other hand, the presence of 1200 or 2400 mg/L $MgSO_4$ mostly or completely stopped Mn(II) oxidation by *Ps. putida* MnB1, respectively (Figure 5b), even in the presence of Cu(II).

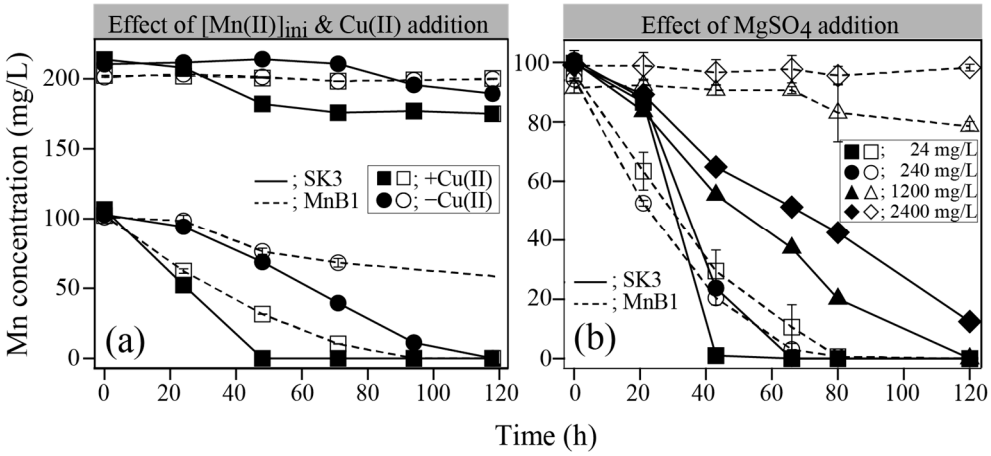

Figure 5. Mn(II) oxidative removal by isolate SK3 (solid symbols with solid lines) in comparison with *Ps. putida* MnB1 (open symbols with broken lines) under different conditions (pH_{ini} 7.0, 25 °C). (**a**) Effects of the initial Mn(II) concentration (100 or 200 mg/L) was tested in the presence (■, □) or absence (●, ○) of 3 μM Cu(II). [$MgSO_4$] = 24 mg/L (present originally in PYG-1 medium). (**b**) Effects of increasing dose of $MgSO_4$ was tested by adding extra $MgSO_4$ to a final concentration of 240 mg/L (●, ○), 1200 mg/L (▲, △) or 2400 mg/L (◆, ◇), in comparison with the controls (■, □; 24 mg/L $MgSO_4$ originally present in PYG-1 medium). [Mn^{2+}] = 100 mg/L. [Cu(II)] = 3 μM.

3.4.2. Effect of pH and temperature

Mn(II) oxidation activity by isolate SK3 peaked over the relatively wider pH range (7.0–8.0) when 3 μM Cu(II) was present, whereas the activity of *Ps. putida* MnB1 peaked at pH 7.0 and a slight pH shift, due especially to alkali, caused a detrimental effect (Figure 6a). Chemical Mn(II) oxidation is

thermodynamically unfavorable at acidic pHs for initiation of Mn(II) oxidation coupled with O_2 [1]. However, even at the slightly acidic pH of 6.5, Mn(II) oxidation by isolate SK3 persisted, even with a greater Mn removal rate than that by *Ps. putida* MnB1 at its optimal pH 7.0. Both strains lost their Mn(II) oxidation activity at pH 6.0 (Figure 6a). Interestingly, however, the absence of Cu(II) resulted in total deactivation of Mn(II) oxidation by isolate SK3 at pH 7.5 and 8.0 (Figure 6a). Isolate SK3 showed a clear preference for the temperature of 25 °C, while lower (20 °C) or higher (30 °C) temperatures slowed down Mn(II) oxidation by one-fourth (Figure 6b). On the other hand, the Mn(II) oxidation rate by *Ps. putida* MnB1 was nearly stable over 20–30 °C. Both strains lost Mn(II) oxidation ability at 35 °C (Figure 6b), although no decrease in the cell density was observed (data not shown). Overall, it was clearly shown that under optimal conditions, Mn(II) oxidative removal by isolate SK3 was shown significantly greater than *Ps. putida* MnB1 (Figure 6a,b). The positive effect of Cu(II) in Mn(II) oxidation by isolate SK3 was also emphasized here. Although under the detection limit (Table 1), a small amount of available Cu(II) ions might have facilitated on-site Mn deposition in the wastewater pipe.

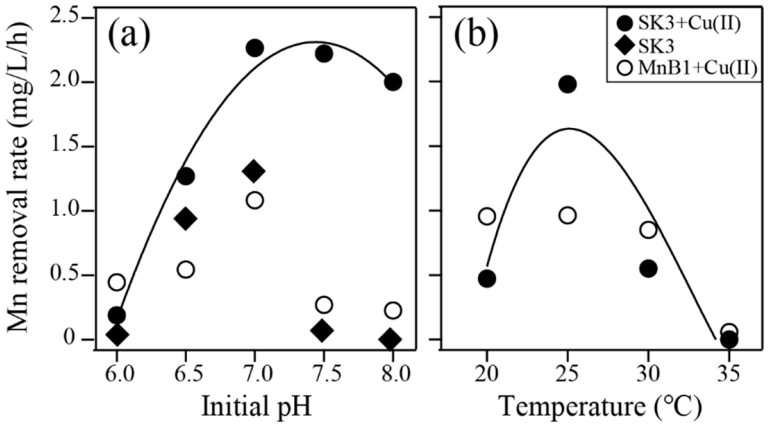

Figure 6. Mn(II) oxidative removal rates at different initial pHs (**a**) and temperatures (**b**). ●, isolate SK3 with 3 μM Cu(II) (calculated for the time period of 0–48 h). ◆, isolate SK3 without Cu(II) (calculated for the time period of 0–63 h). ○, *Ps. putida* MnB1 with 3 μM Cu(II) (calculated for the time period of 0–72 h). Initial conditions: [Mn(II)] = 100 mg/L; [$MgSO_4$] = 24 mg/L (originally present in PYG-1 medium). (**a**) The temperature was set at 25 °C. (**b**) The initial pH was set at 7.0. Fitting curves were drawn only for isolate SK3 with 3 μM Cu(II). The experiments were conducted in duplicate.

3.4.3. Effect of Medium Components

The above Mn(II) oxidation tests under different conditions indicated the potential effectiveness of isolate SK3 (also relative to the representative Mn(II)-oxidizing *Pseudomonas* strain) for industrial application. Therefore, isolate SK3 was further tested for its persistence in the oligotrophic medium by omitting one or more organic components from the PYG-1 medium (Figure 7). Removing glucose caused some delay in Mn(II) oxidation, but no severe effect was seen as long as complex nutrients were provided (Figure 7a). The amount of complex nutrients could be lowered (by removing peptone and, at the same time, halving yeast extract) without altering Mn(II) oxidation activity. However, the total absence of complex nutrients led to a severe decline in cell densities (Figure 7c) and, thus, no Mn(II) oxidation was achieved (Figure 7a). These results indicated that in actual industrial operation, feeding a minimum amount of complex nutrients would be essential to promote oxidative Mn(II) removal. The absence of buffering agent (PIPES) caused a pH drop from 7.0 to 6.0, owing to the proton-generating Mn(II) oxidation reaction ($Mn^{2+} + 1/2\ O_2 + H_2O \rightarrow MnO_2 + 2H^+$) to consequently halt microbial activity. This suggests that the addition of a buffering effect would be necessary to maintain microbial activity when applying to actual industrial wastewaters.

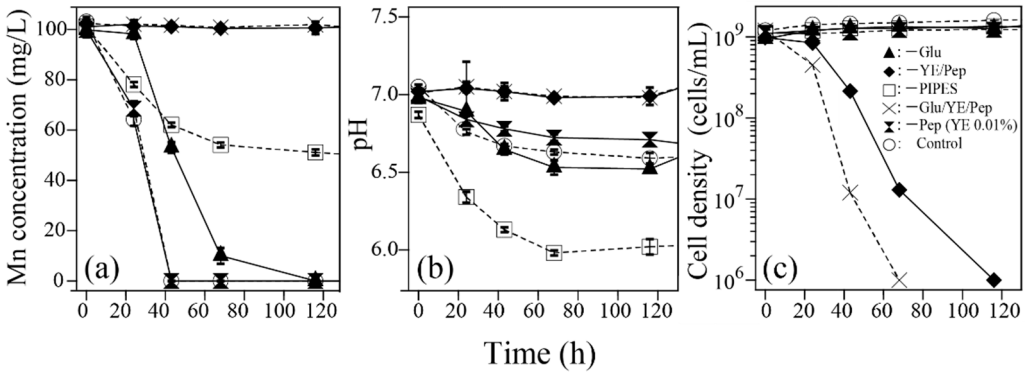

Figure 7. Effect of individual PYG-1 medium components on Mn(II) oxidative removal. Changes in the (**a**) Mn concentration, (**b**) pH value, and (**c**) cell density during Mn(II) oxidation are shown. The following components were omitted from PYG-1 medium: ▲, −Glu; ♦; −YE/Pep; □, −PIPES, ×, −Glu/YE/Pep; ⧗, −Pep (YE lowered to 0.01%); ○, Control (Glu, glucose; YE, yeast extract; Pep, peptone). Initial conditions: [Mn(II)] = 100 mg/L; [Cu(II)] = 3 µM; [$MgSO_4$] = 24 mg/L (originally present in PYG-1 medium) at pH 7.0, 25 °C. The experiments were conducted in duplicate.

3.4.4. Analysis of Biogenic Mn-Oxides Produced by Pseudomonas sp. SK3

The over-time change in XRD peaks of biogenic Mn-oxide precipitates is shown in Figure 8. The broad peak at around 20° deriving from cellular carbon (Figure 8a) gradually became unnoticeable, accompanied by the emergence of increasingly evident birnessite peaks (Figure 8b–d). The mineral surface morphology of biogenic birnessite (Figure 8f) and chemically synthesized acid birnessite (Figure 8g) were compared. A number of bacterial cells were found attached onto the biogenic birnessite surface, hidden in the mineral pores, or encrusted by self-produced Mn-oxides. The surface of the biogenic birnessite was coated with string-like biofilm structures (Figure 8f). The XANES LCF fitting indicated that the over-time maturation of biogenic birnessite (Figure 8 a–d) was accompanied with a change in the Mn oxidation states (Figure 9a). The ratio of Mn(II) and Mn(III) in the birnessite structure steadily decreased during Mn(II) oxidation by isolate SK3, altering the AOS from 3.5 (at 24 h) to 3.8 (at 72 h). A slower Mn(II) oxidation by *Ps. putida* MnB1 compared to isolate SK3 (Figure 5a) was accompanied by a slower change in the Mn AOS (from 3.5 at 24 h to 3.73 at 120 h; Figure 9b). The enhancing effect of Cu(II) on Mn(II) oxidation (observed in 3.4.1–3.4.2) together with the sequential change in the Mn oxidation state of biogenic birnessite observed here, in fact, support the one-electron Mn(II) oxidation reaction suggested for MCO enzymes [38,39].

Chemically synthesized birnessite (such as biogenic birnessite) were reported to undergo structural transformation via the synproportionation reaction between adsorbed Mn(II) and the surrounding Mn(IV), leading to Mn(III) formation, with the Mn AOC shifting from 3.7 to 3.5 in 20 days [40]. This decrease in the Mn AOS of birnessite during mineral ripening results in its deactivation as the chemical oxidant. The oxidative removal of Mn(II) from wastewaters would rely both on microbial (enzymatic) Mn(II) oxidation and chemical Mn(II) oxidation by Mn(IV). Therefore, accumulation and passivation of Mn(III) onto Mn^{IV}-oxides needs to be avoided in order to maintain effective and continuous Mn removal.

The ability of isolate SK3 to effectively raise the Mn AOS to 3.8 (Figure 8a) would therefore be advantageous for steady and continuous water treatment. Together with the efficient in vitro Mn(II) oxidation displayed by isolate SK3, the high Mn AOS level of 3.75 observed with the in situ pipeline Mn-deposit suggests that continuous generation of Mn(IV) was promoted via the robust in situ activity of indigenous Mn(II) oxidizers (including strain SK3). This microbial reaction also likely pushed the chemical Mn(II)/Mn(IV) synproportionation reaction, resulting in synergistic Mn oxidative removal within the complex ecosystem established in this artificial pipeline structure.

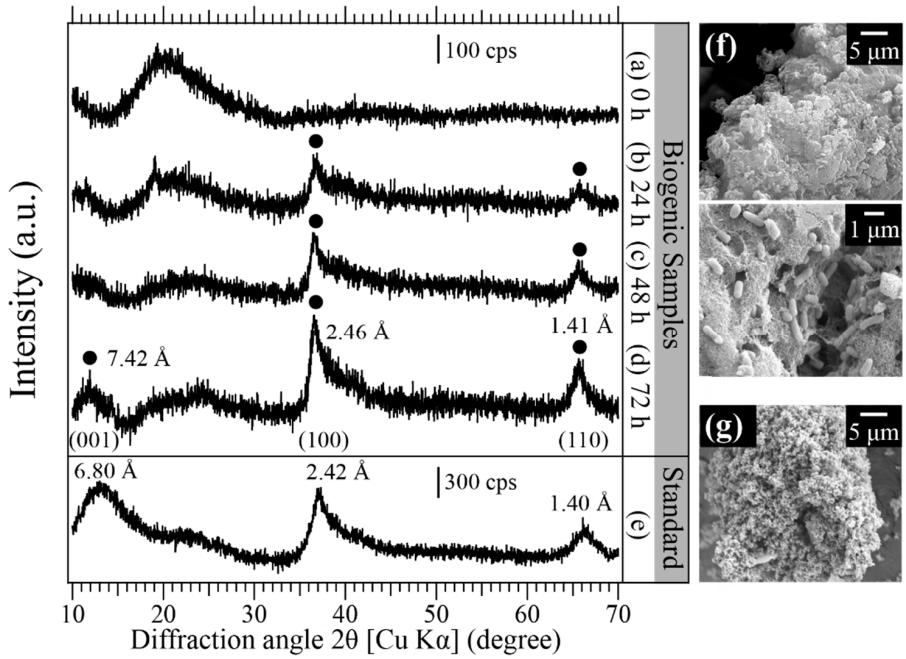

Figure 8. XRD diffraction patterns of Mn-precipitates recovered during Mn(II) oxidation by isolate SK3 at 0 h (**a**), 24 h (**b**), 48 h (**c**), and 72 h (**d**), in comparison with chemically synthesized acid birnessite (**e**). •, birnessite (JCDD 43-1456). Sampling times of the Mn-precipitates correspond to those shown in Figure 5a (■, +Cu(II)). SEM images of sample (**d**) and (**e**) are shown in (**f**) and (**g**), respectively.

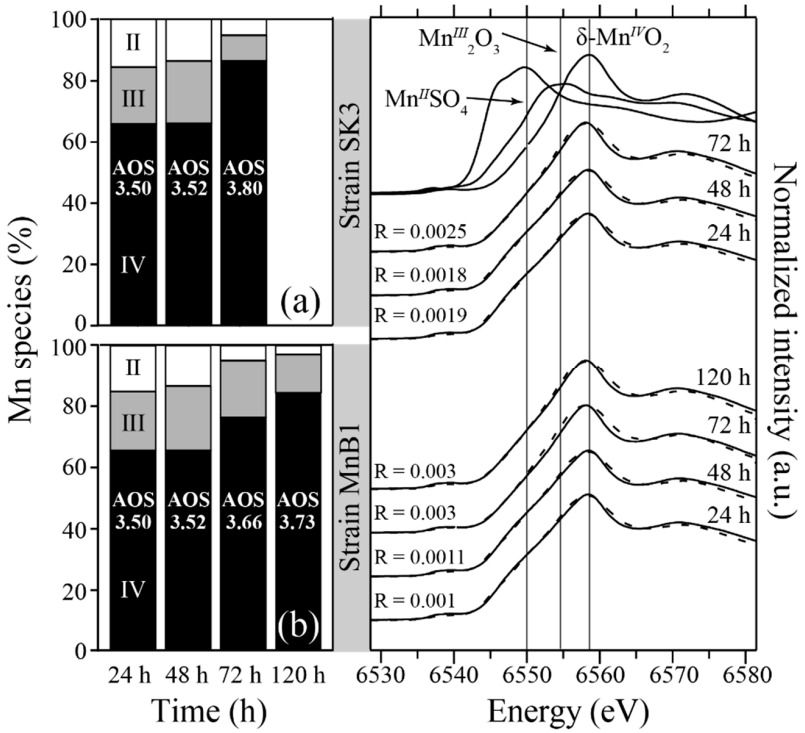

Figure 9. Changes in the Mn AOS of Mn-precipitates produced by isolate SK3 (**a**) or *Ps. Putida* MnB1 (**b**). The ratios of Mn(II) (white), Mn(III) (grey), and Mn(IV) (black) were calculated from the linear combination fitting result (broken lines) of Mn K-edge XANES spectra (solid lines). Sampling points (24, 48, 72, and 120 h) of the Mn-precipitates correspond to those shown in Figure 5a (■ □, +Cu^{2+}). As Mn standards, $Mn^{II}SO_4$, $Mn^{III}{}_2O_3$, and δ-$Mn^{IV}O_2$ were used. AOS stands for average oxidation state. Fitting results with *R*-factors < 0.003 were considered reliable.

Supplementary Materials: The following are available online at http://www.mdpi.com/2073-4441/11/3/507/s1. Figure S1: Bacterial community structure in Mn-deposits collected from the metal refinery wastewater pipe (full data). Table S1: NCBI accession numbers used to construct the phylogenetic tree in Figure 4. Table S2: Species names under the genera *Hyphomicrobium*, *Magnetospirillum*, *Geobacter*, *Bacillus*, and *Pseudomonas* detected in the bacterial community structure shown in Figure 2.

Author Contributions: S.K. and K.T. performed the experiments under the supervision of N.O. S.K. prepared the manuscript draft, which was reviewed and revised by N.O.

Funding: This research received no external funding.

Acknowledgments: The XAFS experiments were performed at the SAGA Light Source (Kyushu University Beam Line; BL06, No. 2016IIIK006). S.K. is grateful for financial assistance provided by the Kyushu University Advanced Graduated Program in Global Strategy for Green Asia.

Conflicts of Interest: The authors declare no conflicts of interest.

References

1. Morgan, J.J. Kinetics of reaction between O_2 and Mn(II) species in aqueous solutions. *Geochim. Cosmochim. Acta* **2005**, *69*, 35–48. [CrossRef]
2. Tebo, B.M.; Bargar, J.R.; Clement, B.G.; Dick, G.J.; Murray, K.J.; Parker, D.; Verity, R.; Webb, S.M. Biogenic manganese oxides: Properties and mechanisms of formation. *Annu. Rev. Earth Planet. Sci.* **2004**, *32*, 287–328. [CrossRef]
3. Tebo, B.M.; Johnson, H.A.; McCarthy, J.K.; Templeton, A.S. Geomicrobiology of manganese(II) oxidation. *Trends Microbiol.* **2005**, *13*, 421–428. [CrossRef] [PubMed]
4. Dick, G.J.; Torpey, J.W.; Beveridge, T.J.; Tebo, B.M. Direct identification of a bacterial manganese(II) oxidase, the multicopper oxidase MnxG, from spores of several different marine Bacillus species. *Appl. Environ. Microbiol.* **2008**, *74*, 1527–1534. [CrossRef] [PubMed]
5. Zeng, X.; Zhang, M.; Liu, Y.; Tang, W. Manganese(II) oxidation by the multi-copper oxidase CopA from *Brevibacillus panacihumi* MK-8. *Enzyme Microb. Technol.* **2018**, *117*, 79–83. [CrossRef] [PubMed]
6. Corstjens, P.L.A.M.; de Vrind, J.P.M.; Goosen, T.; de Vrind-de Jong, E.W. Identification and molecular analysis of the *Leptothrix discophora* SS-1 *mofA* gene, a gene putatively encoding a manganese-oxidizing protein with copper domains. *Geomicrobiol. J.* **1997**, *14*, 91–108. [CrossRef]
7. Francis, C.A.; Tebo, B.M. *cumA* Multicopper Oxidase Genes from Diverse Mn(II)-oxidizing and non-Mn(II)-oxidizing Pseudomonas Strains. *Appl. Environ. Microbiol.* **2001**, *67*, 4272–4278. [CrossRef] [PubMed]
8. Ridge, J.P.; Lin, M.; Larsen, E.I.; Fegan, M.; McEwan, A.G.; Sly, L.I. A multicopper oxidase is essential for manganese oxidation and laccase-like activity in *Pedomicrobium* sp. ACM 3067. *Environ. Microbiol.* **2007**, *9*, 944–953. [CrossRef] [PubMed]
9. Geszvain, K.; Smesrud, L.; Tebo, B.M. Identification of a Third Mn(II) Oxidase Enzyme in *Pseudomonas putida* GB-1. *Appl. Environ. Microbiol.* **2016**, *82*, 3774–3782. [CrossRef] [PubMed]
10. Bohu, T.; Santelli, C.M.; Akob, D.M.; Neu, T.R.; Ciobota, V.; Rosch, P.; Popp, J.; Nietzsche, S.; Kusel, K. Characterization of pH dependent Mn(II) oxidation strategies and formation of a bixbyite-like phase by *Mesorhizobium australicum* T-G1. *Front. Microbiol.* **2015**, *6*, 734. [CrossRef] [PubMed]
11. Mann, S.; Sparks, N.H.; Scott, G.H.; de Vrind-de Jong, E.W. Oxidation of Manganese and Formation of Mn(3)O(4) (Hausmannite) by Spore Coats of a Marine *Bacillus* sp. *Appl. Environ. Microbiol.* **1988**, *54*, 2140–2143. [PubMed]
12. Santelli, C.M.; Webb, S.M.; Dohnalkova, A.C.; Hansel, C.M. Diversity of Mn oxides produced by Mn(II)-oxidizing fungi. *Geochim. Cosmochim. Acta* **2011**, *75*, 2762–2776. [CrossRef]
13. Saratovsky, I.; Gurr, S.J.; Hayward, M.A. The Structure of manganese oxide formed by the fungus *Acremonium* sp. strain KR21-2. *Geochim. Cosmochim. Acta* **2009**, *73*, 3291–3300. [CrossRef]
14. Feng, X.H.; Zhu, M.Q.; Ginder-Vogel, M.; Ni, C.Y.; Parikh, S.J.; Sparks, D.L. Formation of nano-crystalline todorokite from biogenic Mn oxides. *Geochim. Cosmochim. Acta* **2010**, *74*, 3232–3245. [CrossRef]
15. Lefkowitz, J.P.; Rouff, A.A.; Elzinga, E.J. Influence of pH on the reductive transformation of birnessite by aqueous Mn(II). *Environ. Sci. Technol.* **2013**, *47*, 10364–10371. [CrossRef] [PubMed]

16. Okibe, N.; Maki, M.; Sasaki, K.; Hirajima, T. Mn(II)-Oxidizing Activity of *Pseudomonas* sp. Strain MM1 is Involved in the Formation of Massive Mn Sediments around Sambe Hot Springs in Japan. *Mater. Trans.* **2013**, *54*, 2027–2031. [CrossRef]
17. Holm, N.C.; Gliesche, C.G.; Hirsch, P. Diversity and structure of hyphomicrobium populations in a sewage treatment plant and its adjacent receiving lake. *Appl. Environ. Microbiol.* **1996**, *62*, 522–528. [PubMed]
18. Sly, L.I.; Hodgkinson, M.C.; Arunpairojana, V. Effect of Water Velocity on the Early Development of Manganese-Depositing Biofilm in a Drinking-Water Distribution-System. *FEMS Microbiol. Ecol.* **1988**, *53*, 175–186. [CrossRef]
19. Tyler, P.A. Hyphomicrobia and the oxidation of manganesse in aquatic ecosystems. *Antonie Van Leewenhoek* **1970**, *36*, 567–578. [CrossRef]
20. Cheng, Q.; Nengzi, L.; Bao, L.; Huang, Y.; Liu, S.; Cheng, X.; Li, B.; Zhang, J. Distribution and genetic diversity of microbial populations in the pilot-scale biofilter for simultaneous removal of ammonia, iron and manganese from real groundwater. *Chemosphere* **2017**, *182*, 450–457. [CrossRef] [PubMed]
21. Qin, S.Y.; Ma, F.; Huang, P.; Yang, J.X. Fe (II) and Mn (II) removal from drilled well water: A case study from a biological treatment unit in Harbin. *Desalination* **2009**, *245*, 183–193. [CrossRef]
22. Bai, Y.; Chang, Y.; Liang, J.; Chen, C.; Qu, J. Treatment of groundwater containing Mn(II), Fe(II), As(III) and Sb(III) by bioaugmented quartz-sand filters. *Water Res.* **2016**, *106*, 126–134. [CrossRef]
23. Cai, Y.; Li, D.; Liang, Y.; Zeng, H.; Zhang, J. Operational parameters required for the start-up process of a biofilter to remove Fe, Mn, and NH_3-N from low-temperature groundwater. *Desalin. Water Treat.* **2014**, *57*, 3588–3596. [CrossRef]
24. Thompson, J.D.; Gibson, T.J.; Plewniak, F.; Jeanmougin, F.; Higgins, D.G. The CLUSTAL_X Windows Interface: Flexible Strategies for Multiple Sequence Alignment Aided by Quality Analysis Tools. *Nucleic Acids Res.* **1998**, *25*, 4876–4882. [CrossRef]
25. Villalobos, M.; Toner, B.; Bargar, J.; Sposito, G. Characterization of the manganese oxide produced by *Pseudomonas putida* strain MnB1. *Geochim. Cosmochim. Acta* **2003**, *67*, 2649–2662. [CrossRef]
26. Ravel, B.; Newville, M. ATHENA, ARTEMIS, HEPHAESTUS: Data analysis for X-ray absorption spectroscopy using IFEFFIT. *J. Synchrotron Radiat.* **2005**, *12*, 537–541. [CrossRef] [PubMed]
27. Friedl, G.; Wehrli, B.; Manceau, A. Solid phases in the cycling of manganese in eutrophic lakes: New insights from EXAFS spectroscopy. *Geochim. Cosmochim. Acta* **1997**, *61*, 3277. [CrossRef]
28. Bodei, S.; Manceau, A.; Geoffroy, N.; Baronnet, A.; Buatier, M. Formation of todorokite from vernadite in Ni-rich hemipelagic sediments. *Geochim. Cosmochim. Acta* **2007**, *71*, 5698–5716. [CrossRef]
29. Bargar, J.R.; Tebo, B.M.; Bergmann, U.; Webb, S.M.; Glatzel, P.; Chiu, V.Q.; Villalobos, M. Biotic and abiotic products of Mn(II) oxidation by spores of the marine *Bacillus* sp. strain SG-1. *Am. Mineral.* **2005**, *90*, 143–154. [CrossRef]
30. Hiraishi, A.; Yonemitsu, Y.; Matsushita, M.; Shin, Y.K.; Kuraishi, H.; Kawahara, K. Characterization of *Porphyrobacter sanguineus* sp. nov., an aerobic bacteriochlorophyll-containing bacterium capable of degrading biphenyl and dibenzofuran. *Arch. Microbiol.* **2002**, *178*, 45–52. [CrossRef] [PubMed]
31. Tyler, P.A.; Marshall, K.C. Microbial oxidation of manganese in hydro-electric pipelines. *Antonie Van Leewenhoek* **1967**, *33*, 171–183. [CrossRef]
32. Uebayasi, M.; Tomizuka, N.; Kamibayashi, A.; Tonomura, K. Autotrophic Growth of a *Hyphomicrobium* sp. and Its Hydrogenase Activity. *Agric. Biol. Chem. Tokyo* **1981**, *45*, 1783–1790. [CrossRef]
33. Zhang, C.; Meng, X.; Li, N.; Wang, W.; Sun, Y.; Jiang, W.; Guan, G.; Li, Y. Two bifunctional enzymes with ferric reduction ability play complementary roles during magnetosome synthesis in *Magnetospirillum gryphiswaldense* MSR-1. *J. Bacteriol.* **2013**, *195*, 876–885. [CrossRef] [PubMed]
34. Prozorov, T.; Perez Gonzalez, T.; Valverde-Tercedor, C.; Jimenez-Lopez, C.; Yebra-Rodriguez, A.; Körnig, A.; Faivre, D.; Mallapragada, S.; Howse, P.; Bazylinski, D.A.; et al. Manganese Incorporation into Magnetosome Magnetite: Magnetic Signature of Doping. *Eur. J. Mineral.* **2014**, *26*, 457–471. [CrossRef]
35. Zacharoff, L.A.; Morrone, D.J.; Bond, D.R. *Geobacter sulfurreducens* Extracellular Multiheme Cytochrome PgcA Facilitates Respiration to Fe(III) Oxides but Not Electrodes. *Front. Microbiol.* **2017**, *8*, 2481. [CrossRef] [PubMed]
36. Francis, C.A.; Tebo, B.M. Enzymatic Manganese(II) Oxidation by Metabolically Dormant Spores of Diverse Bacillus Species. *Appl. Environ. Microbiol.* **2002**, *68*, 874–880. [CrossRef] [PubMed]

37. Geszvain, K.; McCarthy, J.K.; Tebo, B.M. Elimination of manganese(II,III) oxidation in *Pseudomonas putida* GB-1 by a double knockout of two putative multicopper oxidase genes. *Appl. Environ. Microbiol.* **2013**, *79*, 357–366. [CrossRef] [PubMed]
38. Solomon, E.I.; Sundaram, U.M.; Machonkin, T.E. Multicopper Oxidases and Oxygenases. *Chem. Rev.* **1996**, *96*, 2563–2606. [CrossRef] [PubMed]
39. Webb, S.M.; Dick, G.J.; Bargar, J.R.; Tebo, B.M. Evidence for the presence of Mn(III) intermediates in the bacterial oxidation of Mn(II). *Proc. Natl. Acad. Sci. USA* **2005**, *102*, 5558–5563. [CrossRef] [PubMed]
40. Zhao, H.; Zhu, M.; Li, W.; Elzinga, E.J.; Villalobos, M.; Liu, F.; Zhang, J.; Feng, X.; Sparks, D.L. Redox Reactions between Mn(II) and Hexagonal Birnessite Change Its Layer Symmetry. *Environ. Sci. Technol.* **2016**, *50*, 1750–1758. [CrossRef] [PubMed]